

Gradients in primary production predict trophic strategies of mixotrophic corals across spatial scales

Fox, Michael D.; Williams, Gareth J.; Johnson, Maggie D.; Radice, Veronica Z.; Zgliczynski, Brian J.; Kelly, Emily L. A.; Rohwer, Forest L.; Sandin, Stuart A.; Smith, Jennifer E.

Current Biology

DOI:

[10.1016/j.cub.2018.08.057](https://doi.org/10.1016/j.cub.2018.08.057)

Published: 05/11/2018

Peer reviewed version

[Cyswllt i'r cyhoeddiad / Link to publication](#)

Dyfyniad o'r fersiwn a gyhoeddwyd / Citation for published version (APA):

Fox, M. D., Williams, G. J., Johnson, M. D., Radice, V. Z., Zgliczynski, B. J., Kelly, E. L. A., Rohwer, F. L., Sandin, S. A., & Smith, J. E. (2018). Gradients in primary production predict trophic strategies of mixotrophic corals across spatial scales. *Current Biology*, 28(21), 3355-3363. <https://doi.org/10.1016/j.cub.2018.08.057>

Hawliau Cyffredinol / General rights

Copyright and moral rights for the publications made accessible in the public portal are retained by the authors and/or other copyright owners and it is a condition of accessing publications that users recognise and abide by the legal requirements associated with these rights.

- Users may download and print one copy of any publication from the public portal for the purpose of private study or research.
- You may not further distribute the material or use it for any profit-making activity or commercial gain
- You may freely distribute the URL identifying the publication in the public portal ?

Take down policy

If you believe that this document breaches copyright please contact us providing details, and we will remove access to the work immediately and investigate your claim.

Title: *Gradients in primary production predict trophic strategies of mixotrophic corals across spatial scales*

Authors: Michael D. Fox^{1,2*}, Gareth J. Williams³, Maggie D. Johnson⁴, Veronica Z. Radice⁵, Brian J. Zgliczynski¹, Emily L.A. Kelly¹, Forest L. Rohwer⁶, Stuart A. Sandin¹, Jennifer E. Smith¹

¹Center for Marine Biodiversity and Conservation, Scripps Institution of Oceanography, University of California San Diego, La Jolla, CA, 92037 USA

²Lead contact

³School of Ocean Sciences, Bangor University, Anglesey LL59 5AB, UK

⁴Smithsonian Marine Station, Fort Pierce, FL, 34949 USA

⁵Global Change Institute, Australian Research Council Centre of Excellence for Coral Reef Studies, University of Queensland, St. Lucia 4072, QLD, Australia

⁶Department of Biology, San Diego State University, San Diego, CA, 92182 USA

***Correspondence:** fox@ucsd.edu

SUMMARY

Mixotrophy is among the most successful nutritional strategies in terrestrial and marine ecosystems. The ability of organisms to supplement primary nutritional modes along continua of autotrophy and heterotrophy fosters trophic flexibility that can sustain metabolic demands under variable or stressful conditions. Symbiotic, reef-building corals are among the most broadly distributed and ecologically important mixotrophs, yet we lack a basic understanding of how they modify their use of autotrophy and heterotrophy across gradients of food availability. Here we evaluate how one coral species, *Pocillopora meandrina*, supplements autotrophic nutrition through heterotrophy within an archipelago, and test if this pattern holds across species globally. Using stable isotope analysis ($\delta^{13}\text{C}$) and satellite-derived estimates of nearshore primary production (chlorophyll-*a*, as a proxy for food availability), we show that *P. meandrina* incorporates a greater proportion of carbon via heterotrophy when more food is available across five central Pacific islands. We then show that this pattern is consistent globally using data from 15 coral species across 16 locations spanning the Caribbean, Indian, and Pacific Oceans. Globally, surface chlorophyll-*a* explains 77% of the variation in coral heterotrophic nutrition, 86% for one genus across 10 islands, and 94% when controlling for coral taxonomy within archipelagos. These results demonstrate, for the first time, that satellite-derived estimates of nearshore primary production provide a globally relevant proxy for resource availability that can explain variation in coral trophic ecology. Thus, our model provides a pivotal step towards resolving the biophysical couplings between mixotrophic organisms and spatial patterns of resource availability in the coastal oceans.

Key Words: Coral reef, Heterotrophy, Stable Isotopes, Phytoplankton, Nutrients, Chlorophyll-*a*, Oceanography, Remote Sensing

INTRODUCTION

Mixotrophic organisms can balance their reliance on different nutritional modes (i.e., autotrophy and heterotrophy) in accordance with spatiotemporal fluctuations in resource availability. This trophic flexibility allows mixotrophs to adapt to a wide range of terrestrial and aquatic biomes, making mixotrophy one of the most ubiquitous nutritional strategies on earth [1]. Most mixotrophs subsist along a continuum of autotrophy and heterotrophy, such as vascular plants that can supplement autotrophic nutrition along gradients of limiting resources through carnivory or mycoheterotrophy [2, 3]. Dynamic marine environments favor mixotrophic organisms, which are broadly distributed and provide crucial linkages for energy flow between trophic levels [4]. Many cnidarians and sponges have evolved a tight symbiosis with microalgae to sustain high rates of primary production in oligotrophic regions [5, 6]. Of these animals, mixotrophic reef-building corals form the foundation of one of the most biodiverse and productive marine ecosystems, yet our understanding of how corals adjust nutritional modes in response to natural gradients in resource availability (e.g., inorganic nutrients and particulate resources) remains limited [7]. Given their pantropical distribution, mixotrophic corals represent an opportunity to examine the biophysical coupling between resource availability and the trophic ecology of mixotrophic organisms across spatial scales.

Reef-building corals obtain energy from both autotrophy, via their endosymbiotic microalgae of the genus *Symbiodinium*, and heterotrophy via the capture of allochthonous particles [8]. While the physiological benefits of this trophic plasticity were acknowledged by early studies of coral biology [5], the ecological success of scleractinian corals has long been attributed to their symbiotic nature [9]. Indeed, photosynthetically fixed carbon translocated from endosymbionts to the coral host can contribute more than 100% of the daily metabolic

requirements of corals [10-12]; however much of the fixed carbon is respired or released as mucus rather than incorporated into host biomass [13, 14]. Heterotrophy on the other hand, provides corals with carbon and essential nutrients (e.g., nitrogen and phosphorus) that directly support growth and reproduction [15, 16]. The physiological importance of heterotrophy for corals is widely accepted, yet a disproportionate amount of research to date has focused on the role of endosymbionts in defining coral nutrition [7].

Heterotrophic nutrition can mitigate the negative effects of environmental stressors on coral physiology. For example, heterotrophy can increase coral recovery rates following acute stress, decrease overall mortality, and help reestablish the coral-algal symbiosis following thermally-induced bleaching [11, 17-19]. Heterotrophic nutrition can increase coral fecundity [15] and also facilitate calcification under low pH conditions, which is critical for coral growth and therefore the structural development and persistence of reefs through time [20, 21]. *In situ*, increased rates of heterotrophy by corals are often considered a response to the contrasting gradients of light and resource availability [22] and are thought to increase with depth [23]. However, some corals may feed continuously across depth in areas where heterotrophic resources are more abundant [24, 25]. Food availability for corals is linked with nearshore primary production (PP_n) [26]. Thus future reductions in PP_n , caused by increased ocean stratification [27] and moderate to strong El Niño events [28] likely represent an unanticipated stressor on the persistence of coral populations in a warming ocean. Understanding the relationship between PP_n and coral trophic ecology will improve our capacity to accurately predict the implications of global change on coral populations over space and time.

To date, our understanding of heterotrophic nutrition in corals is largely laboratory-based [7, 14, 16, 19, 29, 30], thus limiting our ability to assess coral feeding at broader, more

ecologically relevant scales. New techniques are required to propel our understanding of coral nutrition beyond individual colonies and to scale these patterns up to entire reef ecosystems. An essential first step is to link regional variation in environmental conditions with the biological responses of corals. Remotely sensed estimates of surface chlorophyll-*a* (chl-*a*) [31] have revealed significant increases in phytoplankton biomass in the nearshore regions of oceanic islands across the Pacific [26]. Notably, these satellite-derived chl-*a* estimates are correlated strongly with PP_n throughout the photic zone as well as the relative abundance of zooplankton, a primary food resource for corals [32, 33]. Remotely sensed surface chl-*a* may therefore provide a globally relevant proxy for estimating PP_n and heterotrophic resource availability on coral reefs. Similarly, stable isotope analyses ($\delta^{13}\text{C}$ and $\delta^{15}\text{N}$) of coral hosts and their endosymbionts can assess the relative contributions of heterotrophic and autotrophic nutrition across multiple coral species and spatial scales [18, 23, 24].

To test for a link between heterotrophic resource availability and the trophic response of mixotrophic corals, we compared the $\delta^{13}\text{C}$ and $\delta^{15}\text{N}$ values of corals to satellite-derived estimates of PP_n (using chl-*a* as a proxy for plankton biomass). At an archipelago scale, we measured the degree of heterotrophy in a common reef-building coral (*Pocillopora meandrina*) collected across depths (5-30 m) at five uninhabited islands in the Southern Line Islands of Kiribati (SLI) and modeled these against concurrent changes in PP_n. To determine if the same relationship held globally, we synthesized published $\delta^{13}\text{C}$ and $\delta^{15}\text{N}$ values for 15 coral species from 16 locations across the Red Sea, Caribbean, Indian and Pacific Oceans and modeled these against climatological estimates of PP_n for each location.

RESULTS

Oceanographic context of the Southern Line Islands (SLI)

The oceanic primary production gradient across the SLI is conspicuous, with climatological surface chl-*a* concentrations (2004-2015) separating the islands into distinct regions (Figure 1A, 1B). Surface chl-*a* (a proxy for PP_n) was similar at the three southern islands (Flint, Vostok, and Millennium) while considerably higher and with less inter-annual variation at the northern two (Starbuck and Malden) ($F_{4,55} = 27.48$, $p < 0.01$; Tukey HSD: FLI, VOS, MIL < STA, MAL). The mean depth of light penetration at 490 nm (a proxy for light attenuation) from 2004-2015 ranged from 29-35 m, which suggests the light environment on these islands does not differ markedly on decadal time scales. Inorganic nutrient concentrations were latitude-dependent and closely associated with the chl-*a* gradient (Figure 1C). Mean dissolved inorganic nitrogen (DIN) concentrations increased nine-fold (0.51-4.69 μmol) from south to north with a concomitant increase in soluble reactive phosphorus (SRP) (0.15-0.44 μmol , $F_{4,40} = 70.66$, $p < 0.01$). Within islands, inorganic nutrient concentrations were homogenous in the upper 30 m and consistent with measurements from 2009 [34]. During our study, *in situ* irradiance was similar throughout the SLI and there was no pattern between islands (i.e., the more productive islands did not have reduced irradiance relative to the more oligotrophic islands). On sunny days, mean daily irradiance ranged from 374-546 $\mu\text{E m}^{-2} \text{ s}^{-1}$ and total integrated daily irradiance ranged from 11.76-17.04 $\text{E m}^{-2} \text{ d}^{-1}$.

Coral and endosymbiont $\delta^{15}\text{N}$ values were influenced most strongly by location due to a baseline shift in $\delta^{15}\text{N}$ of nitrate that occurs along the oceanic primary production gradient in the equatorial Pacific (lower $\delta^{15}\text{N}$ values closer to the equator) [35]. As a result, coral and endosymbiont $\delta^{15}\text{N}$ decreased from Flint to Malden. The endosymbiont fraction became more deplete in ^{15}N with depth at all islands while coral host $\delta^{15}\text{N}$ only declined with depth on

Starbuck (Tables S1, S2). C:N values were elevated in the coral host fraction on Starbuck and Malden, which indicates the nitrogen content of the coral and endosymbiont fractions did not increase along the nutrient gradient (Table S1). However, the overall chl-*a* content of *P. meandrina* endosymbionts increased from Flint to Malden (Island: $F_{(4,60)} = 21.26$, $p < 0.01$, TukeyHSD: FLI < VOS, MIL, STA < MAL). Pigment content generally increased from 10-30 m but was highly variable (Depth: $F_{(2,60)} = 6.61$, $p < 0.01$, TUKEY HSD: 10m < 30 m, Figure S1). Endosymbiont density was positively correlated with chl-*a* content at 10 m depth across all islands (Pearson's correlation: $t_{(1,25)} = 5.27$, $p < 0.01$, $r = 0.73$).

Isotopic evidence for coral heterotrophy across islands and depth

The $\delta^{13}\text{C}$ values of coral and endosymbiont tissues can be influenced by differences in photosynthetic rates (autotrophic nutrition) and by the incorporation of allochthonous food sources via particle capture (referred to herein as heterotrophic carbon). Decreased rates of photosynthetic fractionation cause coral host and endosymbiont $\delta^{13}\text{C}$ values to decrease with depth [23]. Planktonic communities and POM are the primary heterotrophic resources for corals. On most coral reefs these resources are depleted in ^{13}C (more negative $\delta^{13}\text{C}$) relative to *Symbiodinium* spp. by at least 4-6 ‰ [25]. Thus, increased heterotrophic nutrition leads to a reduction in coral host $\delta^{13}\text{C}$ values. The relative difference between the coral host and endosymbiont $\delta^{13}\text{C}$ ($\Delta^{13}\text{C} = \delta^{13}\text{C}_{\text{host}} - \delta^{13}\text{C}_{\text{endosymbiont}}$) can therefore be used to disentangle the relative effects of photosynthetic fractionation and incorporation of heterotrophic carbon. While not a quantitative estimate of the heterotrophic contribution to a corals metabolic demands, this isotopic proxy ($\Delta^{13}\text{C}$) provides insight to deviations from a fully autotrophic diet and reliably tracks intra-island gradients in resource availability [18, 23, 24].

Coral host and endosymbiont $\delta^{13}\text{C}$ values declined linearly with depth and $\delta^{13}\text{C}$ for both fractions ranged from -14 to -18 ‰ across the SLI (Figure 1A-E, Table S1). Host $\delta^{13}\text{C}$ was consistently lower than the endosymbiont fraction and was greatest at Flint (southernmost island) and lowest at Malden (northernmost). In contrast, endosymbiont $\delta^{13}\text{C}$ did not vary among islands. As an additional proxy of coral heterotrophy we also examined the relative similarity of coral host $\delta^{13}\text{C}$ and the mean $\delta^{13}\text{C}$ of the reef associated zooplankton at each island ($\Delta^{13}\text{C}_{\text{host-zooplankton}} = \delta^{13}\text{C}_{\text{host}} - \delta^{13}\text{C}_{\text{zooplankton}}$). Coral host $\delta^{13}\text{C}$ values became more similar to zooplankton $\delta^{13}\text{C}$ (more depleted in ^{13}C , lower $\Delta^{13}\text{C}_{\text{host-zooplankton}}$) with increasing surface chl-*a*, indicating a greater incorporation of heterotrophic carbon at the more productive islands ($\Delta^{13}\text{C}_{\text{host-zooplankton}} - F_{(1,3)} = 44.89$, $p = <0.01$, $r^2 = 0.94$, Figure 1D). There was no relationship between coral and zooplankton $\delta^{15}\text{N}$ ($\Delta^{15}\text{N}_{\text{host-zooplankton}} - F_{(1,3)} = 0.97$, $p = 0.65$).

In contrast to the individual $\delta^{13}\text{C}$ values of the corals and endosymbiont tissues, $\Delta^{13}\text{C}$ ($\delta^{13}\text{C}_{\text{host}} - \delta^{13}\text{C}_{\text{endosymbiont}}$) varied as a function of chl-*a* across the SLI (Figure 2F-J, Table S1). *P. meandrina* $\Delta^{13}\text{C}$ was most negative on islands with higher surface chl-*a*. On Flint and Vostok (most oligotrophic), *Pocillopora* exhibited increased reliance on heterotrophic carbon sources (more negative $\Delta^{13}\text{C}$) as a function of depth (from 5 to 30 m depth: Flint: slope = -0.23, $p < 0.01$, $r^2 = 0.97$ Vostok: slope = -0.19, $p = 0.05$, $r^2 = 0.67$, Figure 2I, 2J, Table S1). There was no depth dependence of $\Delta^{13}\text{C}$ on Millennium, Starbuck, or Malden (Figure 2F, 2G, 2H). Importantly, $\Delta^{13}\text{C}$ was not related to coral surface area normalized chl-*a* concentrations (Pearson's correlation: $t_{(1,25)} = -1.89$, $p = 0.2$, $r = 0.1$) or endosymbiont densities ($t_{(1,25)} = 1.65$, $p = 0.2$, $r = 0.25$).

Coral $\Delta^{15}\text{N}$ and $\Delta\text{C:N}$ values showed no consistent relationships with islands or depth (Table S2). $\Delta^{15}\text{N}$ values on Millennium were similar with those of Flint and Vostok but did not increase with depth. On Starbuck and Malden, $\Delta^{15}\text{N}$ values were generally lower and did not

vary with depth. Coral $\Delta C:N$ was highest on Starbuck and Malden indicating greater concentrations of lipids in the animal fraction on the more productive islands.

Global patterns of coral $\delta^{13}C$ and $\delta^{15}N$ in relation to nearshore primary production

Coral $\delta^{13}C$ and $\delta^{15}N$ values vary with large-scale physical processes but $\Delta^{13}C$ is most tightly coupled with surface chl-*a* across 16 locations spanning three ocean basins. Latitude was positively related to coral and endosymbiont $\delta^{13}C$, respectively, but this relationship did not explain a significant amount of variation due to the low $\delta^{13}C$ values of *Madracis auretenra* on Curaçao (Figure S2, Table S4). Latitude was unrelated to $\Delta^{13}C$. Coral and endosymbiont $\delta^{15}N$ showed no coherent pattern when considered globally (Table S4). However, considering only *Pocillopora*, host and endosymbiont $\delta^{15}N$ (but not $\Delta^{15}N$) were well explained by latitude, chl-*a*, and estimated thermocline depth (Table S4). $\delta^{15}N$ values were lowest in regions with shallower thermoclines and higher chl-*a*.

Coral and endosymbiont $\delta^{13}C$ values were tightly constrained across species and geography and did not vary as a function of surface chl-*a* (Figure 3A-C, Table S2, S3). In contrast, surface chl-*a* explained 77% of the variation in mean coral $\Delta^{13}C$ across 16 locations ($F_{(1,14)} = 46.24$, $r^2 = 0.77$, $p < 0.01$, Figure 3D, Table S3). Additionally, depth of the 22° isotherm (a proxy for thermocline depth) explained 51-69% of the variation in coral $\Delta^{13}C$ (Figure S2, Table S4). Our findings indicate that mixotrophic corals incorporate a greater proportion of heterotrophic carbon (more negative $\Delta^{13}C$) in regions where resource abundance is enhanced by shallower thermoclines and higher surface chl-*a* concentrations.

The linear relationship between $\Delta^{13}C$ and surface chl-*a* is globally consistent, irrespective of taxonomic resolution or spatial scale. For all species, coral or endosymbiont $\delta^{13}C$ values showed no relationship to chl-*a* but $\Delta^{13}C$, while variable, declined significantly with increased

chl-*a* (Tables S2, S3). This relationship was similar when constrained to an archipelago scale (islands within the same region averaged together) to account for potential geographic sampling biases ($F_{(1,5)} = 18.35$, $p = 0.01$, $r^2 = 0.79$). Controlling for four coral families common to all islands, surface chl-*a* remained a significant predictor but explained less variation than the original model at an island-scale ($F_{(1,14)} = 19.04$, $p < 0.01$, $r^2 = 0.58$). When we controlled for coral taxonomy within archipelagos this model explained much more variation ($F_{(1,5)} = 74.31$, $p < 0.01$, $r^2 = 0.94$). Across seven additional linear models that varied by total species number and sampling location, the slope of our observed relationship varied by 6% and explained 70-86% of the overall variation in coral $\Delta^{13}\text{C}$ (Table S3). Coral host $\delta^{13}\text{C}$ was only related to surface chl-*a* in the two most simplified models and endosymbiont $\delta^{13}\text{C}$ was not related to surface chl-*a* in any model. Notably, surface chl-*a* explained 86% of the variation in *Pocillopora spp.* $\Delta^{13}\text{C}$ alone from the Maldives and central Pacific with a similar slope and intercept to the global model (Table S3).

DISCUSSION

Mixotrophic corals benefit greatly from heterotrophic nutrition but the role of oceanographic processes in structuring food availability, and the associated responses of corals, have not been widely studied [24, 36, 37]. Our results indicate the trophic ecology of some corals is spatially flexible, such that corals will increase their use of heterotrophic nutrition when resources are abundant. Specifically, we provide empirical evidence that spatial gradients in nearshore primary production (PP_n) around coral reef islands can directly influence the nutritional status of mixotrophic corals on shallow reefs. Most importantly, we demonstrate that heterotrophic carbon incorporation ($\Delta^{13}\text{C} = \delta^{13}\text{C}_{\text{host}} - \delta^{13}\text{C}_{\text{endosymbiont}}$) is related to surface

chlorophyll-*a* (chl-*a*) at a global scale for multiple coral species across three oceans. We also illustrate that PP_n gradients can influence coral trophic ecology across islands and archipelagos. Our findings support the recent observation that seabird-vectored nutrients may stimulate PP_n and subsequently enhance the growth and biomass of coral reef fish populations [38]. Notably, our study is the first to link patterns of PP_n with the nutrition of coral communities (Figure 3), which provides further evidence that variation in PP_n has strong implications for coral reef ecosystem functioning at multiple scales and trophic levels.

Our results support a working model that many corals will increase heterotrophy as a function of food availability. This is not surprising, as feeding in some coral species is nearly constant [16, 39] and heterotrophic nutrition is often a function of prey encounter rather than a necessity driven by metabolic deficit [40]. Consequently, patterns of PP_n likely have significant influence on the nutritional status and energetic budgets of coral populations. Based on the strong agreement of our statistical analyses with this process-based model, we conclude that the nutritional status of mixotrophic corals is tightly coupled with patterns of PP_n on a global scale. Specifically, using surface chl-*a* as a proxy for PP_n we were able to estimate the $\Delta^{13}\text{C}$ value of multiple coral species at 10 m depth. For example, $\Delta^{13}\text{C}$ values were highly variable among thirteen species of coral from Jamaica (Table S2) [23], but when considered together, the mean $\Delta^{13}\text{C}$ converged on the value predicted by our linear regression. In another example, this relationship captured large seasonal variations in $\Delta^{13}\text{C}$ reported for *Orbicella faveolata* in the northern Florida Keys at 8 m depth [41]. Using the climatological mean chl-*a* for this region (0.21 mg chl-*a* m⁻³), our model was able to approximate the inter-annual mean $\Delta^{13}\text{C}$ (-1.1 ‰) reported by [41] within the error bounds of the linear regression ($\Delta^{13}\text{C} = 0.6$ to -1.1‰). We acknowledge that this relationship may not be relevant for all species, as corals demonstrate

diverse nutritional strategies [29, 39, 42] and differential feeding responses under stressful conditions [11, 43]. Furthermore, the relationship described here cannot resolve all variation in coral $\Delta^{13}\text{C}$ driven by changes in metabolic demands associated with seasonality or environmental conditions (e.g., temperature, light, nutrients) [22]. This implies that the capacity of our model to predict coral trophic strategies will likely improve with the inclusion of additional environmental parameters. For example, in regions of strong seasonal upwelling, large drops in temperature can lower coral metabolic rates and suppress feeding during times of increased food availability [37]. Most importantly, our results show that the relationship between $\Delta^{13}\text{C}$ and surface chl-*a* is effectively constant, whether for a single species (*P. meandrina*) or a global composite of $\Delta^{13}\text{C}$ means derived from 15 species across 16 locations [24, 44].

Our findings also provide strong evidence that at smaller spatial scales (islands and archipelagos) PP_n can influence how a common coral species relies on heterotrophic nutrition across depths. In oligotrophic waters, corals primarily subsist on autotrophy in the particulate-deplete but well-illuminated shallows (more positive $\Delta^{13}\text{C}$) and supplement with heterotrophy as particulate resource availability increases with depth [23, 24, 37, 44]. Consistent with this expectation, heterotrophic nutrition in *P. meandrina* increased with depth (more negative $\Delta^{13}\text{C}$) on the least productive islands in the SLI (Flint and Vostok). In more productive regions, deep-water internal waves frequently deliver inorganic nutrients and planktonic biomass from below the thermocline [44, 45], leading to increased surface chl-*a* and greater food availability at shallower depths [26, 33, 46]. Our results indicate that *P. meandrina* consumed more heterotrophic carbon (more negative $\Delta^{13}\text{C}$) across all depths on Millennium, Starbuck and Malden. This reduction in $\Delta^{13}\text{C}$ was driven by greater incorporation of carbon from zooplankton by the coral host (lower $\Delta^{13}\text{C}_{\text{coral-zooplankton}}$). Coral C:N ratios also increased, consistent with

greater lipid content from heterotrophy in the host tissue, which can play an important role in coral resistance to and recovery following bleaching [47]. In contrast, $\delta^{15}\text{N}$ values did not show consistent patterns across the SLI, suggesting that these changes in heterotrophy may be rather small in the context of the overall nutritional budget of the corals. Thus, $\delta^{13}\text{C}$ may be a more informative proxy for detecting subtle changes in coral nutrition.

Satellite-derived estimates of PP_n provide useful estimates of food availability for shallow water corals, however these estimates do not capture all of the processes that influence food abundance and distribution on a given reef. For example, the $\Delta^{13}\text{C}$ values on Millennium did not vary with depth as expected based on surface chl-*a* concentrations alone (chl-*a* concentrations similar to Flint and Vostok, Figure 1A). As the only atoll in the SLI, Millennium possesses a lagoon that exchanges water with the reef and the flushing of productive lagoon waters can influence PP_n [26]. Notably, spatially explicit downwelling of zooplankton-rich water from Palmyra Atoll's lagoon interacts with internal waves to homogenize food availability across depths, leading to static $\Delta^{13}\text{C}$ values in *P. meandrina* from 10-30 m [24] and we hypothesize this is what is occurring at Millennium. Thus, where *inter*- and *intra*-island physical processes increase heterotrophic resources or re-distribute them throughout the water column, corals may feed opportunistically regardless of depth [17, 24].

To date, the physiological benefits of heterotrophic nutrition in corals have largely been determined in laboratory experiments (reviewed in [48]), though several studies have linked *in situ* feeding with resistance to and recovery following bleaching [11, 17]. As such, corals on reefs with elevated PP_n and greater access to heterotrophic resources may have a greater capacity to survive and recover from acute disturbances [49, 50]. On some coastal reefs, anthropogenic nutrient pollution can increase chl-*a* concentrations [51] and, more importantly, disrupt nitrogen

to phosphorus ratios (N:P) which can increase bleaching sensitivity in corals [52]. Our study identified 16 locations that span a three-fold gradient of naturally elevated surface chl-*a* (0.09-0.29 mg chl-*a* m⁻³) yet the highest values are 1.5-6 times lower than concentrations associated with increased bleaching sensitivity (>0.45 mg chl-*a* m⁻³) [53] and reduced species diversity in polluted locations (2 mg chl-*a* m⁻³) [54]. Thus, although in some coastal or more heavily impacted regions coral resistance to bleaching may not be correlated with surface chl-*a*, for many reefs slightly elevated chl-*a* likely confers benefits [55]. Future work to disentangle the roles of heterotrophic nutrition and background nutrient levels to coral persistence at will be valuable for refining projected coral reef trajectories in a warming ocean.

In conclusion, our study provides the first empirical evidence that coral trophic strategies track nearshore primary production (PP_n) at multiple spatial scales. Our established relationship between coral nutrition ($\Delta^{13}\text{C}$) and surface chl-*a* has high explanatory power and is based on freely available data. Importantly, our model can be applied to coral trophic ecology throughout the tropics because this metric of PP_n is globally comprehensive. Previous investigations of upwelling and PP_n on coral reefs have focused on the role of cooler, upwelled water to moderate temperatures and thus promote coral resistance to bleaching [56-59]. Given the strong connection between coral nutrition and PP_n described here, the contribution of heterotrophy to coral recovery from bleaching has likely been underestimated in areas of naturally elevated PP_n. As such, our model provides a framework to evaluate the importance of heterotrophy to the resilience of coral populations across regions with different background PP_n. This information is essential for improving estimates of the response of corals, and other mixotrophic communities, to predicted variations in PP_n in an era of global change.

Acknowledgements

We are grateful to the Environment and Conservation Division of the Republic of Kiribati for allowing us to conduct research within the Southern Line Islands. The authors thank the owner, captain, and crew of the M/Y Hanse Explorer for logistical support and field assistance. We also thank Jessica Glanz, Ellis Juhlin, Spencer Breining-Aday, Annika Vawter, and Ellen Williams for assistance in the lab. We thank the Moore Family Foundation, the Scripps family and several anonymous donors for their generous financial support. Finally, we are grateful to three anonymous reviewers for their time and valuable comments that have helped to improve this manuscript. VZR collected data from the Maldives with support from the XL Catlin Seaview Survey, funded by XL Catlin and the University of Queensland. MDF was supported by a Nancy Foster Scholarship from the NOAA Office of National Marine Sanctuaries.

Author contributions

Conceptualization: M.D.F., G.J.W., and J.E.S.; Methodology: M.D.F.; Investigation: M.D.F., M.D.J., V.Z.R., B.J.Z, E.L.A.K., and J.E.S.; Writing – Original Draft: M.D.F, G.J.W., and J.E.S.; Writing – Review and Edits: All authors; Funding Acquisition: F.L.R., J.E.S., S.A.S.; Supervision: B.J.Z., F.L.R., J.E.S., S.A.S.

Declaration of Interests

The authors declare no competing interests.

References

1. Selosse, M.-A., Charpin, M., and Not, F. (2016). Mixotrophy everywhere on land and in water: the grand écart hypothesis. *Ecol. Lett.*, doi: 10.1111/ele.12714.
2. Ellison, A.M., and Gotelli, N.J. (2002). Nitrogen availability alters the expression of carnivory in the northern pitcher plant, *Sarracenia purpurea*. *Proc. Natl. Acad. Sci. USA.* 99, 4409-4412.
3. Matsuda, Y., Shimizu, S., Mori, M., Ito, S.I., and Selosse, M.A. (2012). Seasonal and environmental changes of mycorrhizal associations and heterotrophy levels in mixotrophic *Pyrola japonica* (Ericaceae) growing under different light environments. *Am. J. Bot.* 99, 1177-1188.
4. Stoecker, D.K., Hansen, P.J., Caron, D., A. , and Mitra, A. (2017). Mixotrophy in the Marine Plankton. *Ann. Rev. Mar. Sci.* 9, 311-335.
5. Muscatine, L., and Porter, J.W. (1977). Reef corals: mutualistic symbioses adapted to nutrient-poor environments. *Bioscience* 27, 454-460.
6. Venn, A.A., Loram, J.E., and Douglas, A.E. (2008). Photosynthetic symbioses in animals. *J. Exp. Bot.* 59, 1069-1080.
7. Ferrier-Pagès, C., Hoogenboom, M., and Houlbrèque, F. (2011). The role of plankton in coral trophodynamics. In *Coral Reefs: an ecosystem in transition*, Z. Dubinsky and N. Stambler, eds. (Netherlands: Springer), pp. 215-229.
8. Furla, P., Allemand, D., Shick, J.M., Ferrier-Pagès, C., Richier, S., Plantivaux, A., Merle, P.-L., and Tambutté, S. (2005). The Symbiotic Anthozoan: A Physiological Chimera between Alga and Animal. *Integrative and Comparative Biology* 45, 595-604.
9. Veron, J.E.N. (1995). *Corals in space and time: the biogeography and evolution of the Scleractinia*, (Cornell University Press).
10. Muscatine, L., McCloskey, L.R., and Marian, R.E. (1981). Estimating the daily contribution of carbon from zooxanthellae to coral animal respiration. *Limnol. Oceanogr.* 26, 601-611.
11. Grottoli, A.G., Rodrigues, L.J., and Palardy, J.E. (2006). Heterotrophic plasticity and resilience in bleached corals. *Nature* 440, 1186-1189.
12. Davies, P.S. (1984). The role of zooxanthellae in the nutritional energy requirements of *Pocillopora eydouxi*. *Coral Reefs* 2, 181-186.
13. Falkowski, P.G., Dubinsky, Z., Muscatine, L., and Porter, J.W. (1984). Light and the bioenergetics of a symbiotic coral. *Bioscience* 34, 705-709.
14. Tremblay, P., Maguer, J.F., Grover, R., and Ferrier-Pagès, C. (2015). Trophic dynamics of scleractinian corals: stable isotope evidence. *J. Exp. Biol.* 218, 1223-1234.
15. Cox, E.F. (2007). Continuation of sexual reproduction in *Montipora capitata* following bleaching. *Coral Reefs* 26, 721-724.
16. Ferrier-Pagès, C., Witting, J., Tambutte, E., and Sebens, K.P. (2003). Effect of natural zooplankton feeding on the tissue and skeletal growth of the scleractinian coral *Stylophora pistillata*. *Coral Reefs* 22, 229-240.
17. Palardy, J.E., Rodrigues, L.J., and Grottoli, A.G. (2008). The importance of zooplankton to the daily metabolic carbon requirements of healthy and bleached corals at two depths. *J. Exp. Mar. Biol. Ecol.* 367, 180-188.

18. Rodrigues, L.J., and Grottoli, A.G. (2006). Calcification rate and the stable carbon, oxygen, and nitrogen isotopes in the skeleton, host tissue, and zooxanthellae of bleached and recovering Hawaiian corals. *Geochem. Cosmochim. Ac.* 70, 2781-2789.
19. Tremblay, P., Gori, A., Maguer, J.F., Hoogenboom, M., and Ferrier-Pagès, C. (2016). Heterotrophy promotes the re-establishment of photosynthate translocation in a symbiotic coral after heat stress. *Sci. Rep.* 6, 38112.
20. Drenkard, E.J., Cohen, A.L., McCorkle, D.C., de Putron, S.J., Starczak, V.R., and Zicht, A.E. (2013). Calcification by juvenile corals under heterotrophy and elevated CO₂. *Coral Reefs* 32, 727-735.
21. Edmunds, P.J. (2011). Zooplanktivory ameliorates the effects of ocean acidification on the reef coral *Porites* spp. *Limnol. Oceanogr.* 56, 2402-2410.
22. Anthony, K.R., and Fabricius, K. (2000). Shifting roles of heterotrophy and autotrophy in coral energetics under varying turbidity *J. Exp. Mar. Biol. Ecol.* 252, 221-253.
23. Muscatine, L., Porter, J.W., and Kaplan, I.R. (1989). Resource partitioning by reef corals as determined from stable isotope composition. I $\delta^{13}\text{C}$ of zooxanthellae and animal tissue vs depth. *Mar. Biol.* 100, 185-193.
24. Williams, G.J., Sandin, S.A., Zgliczynski, B., Fox, M.D., Furby, K., Gove, J.M., Rogers, J.S., Hartmann, A.C., Caldwell, Z.R., Price, N.N., et al. (2018). Biophysical drivers of coral trophic depth zonation. *Mar. Biol.* 165, 60.
25. Alamaru, A., Loya, Y., Brokovich, E., Yam, R., and Shemesh, A. (2009). Carbon and nitrogen utilization in two species of Red Sea corals along a depth gradient: Insights from stable isotope analysis of total organic material and lipids. *Geochem. Cosmochim. Ac.* 73, 5333-5342.
26. Gove, J.M., McManus, M.A., Neuheimer, A.B., Polovina, J.J., Drazen, J.C., Smith, C.R., Merrifield, M.A., Friedlander, A.M., Ehses, J.S., Young, C.W., et al. (2016). Near-island biological hotspots in barren ocean basins. *Nat Commun* 7, 10581.
27. Behrenfeld, M.J., O'Malley, R.T., Siegel, D.A., McClain, C.R., Sarmiento, J.L., Feldman, G.C., Milligan, A.J., Falkowski, P.G., Letelier, R.M., and Boss, E.S. (2006). Climate-driven trends in contemporary ocean productivity. *Nature* 444, 752.
28. Brainard, R.E., Oliver, T., McPhaden, M.J., Cohen, A., Venegas, R., Heenan, A., Vargas-Ángel, B., Rotjan, R., Mangubhai, S., and Flint, E. (2018). Ecological Impacts of the 2015/16 El Niño in the Central Equatorial Pacific. *Bull. Amer. Meteor. Soc.* 99, S21-S26.
29. Hoogenboom, M., Rottier, C., Sikorski, S., and Ferrier-Pagès, C. (2015). Among-species variation in the energy budgets of reef-building corals: scaling from coral polyps to communities. *J. Exp. Biol.* 218, 3866-3877.
30. Houlbrèque, F., Tambutté, E., and Ferrier-Pagès, C. (2003). Effect of zooplankton availability on the rates of photosynthesis, and tissue and skeletal growth in the scleractinian coral *Stylophora pistillata*. *J. Exp. Mar. Biol. Ecol.* 296, 145-166.
31. Gove, J.M., Williams, G.J., McManus, M.A., Heron, S.F., Sandin, S.A., Vetter, O.J., and Foley, D.G. (2013). Quantifying climatological ranges and anomalies for Pacific coral reef ecosystems. *PLoS ONE* 8, e61974.
32. Croll, D.A., Marinovic, B., Benson, S., Chavez, F.P., Black, N., Ternullo, R., and Tershy, B.R. (2005). From wind to whales: trophic links in a coastal upwelling system. *Mar. Ecol. Prog. Ser.* 289, 117-130.

33. Hazen, E.L., and Johnston, D.W. (2010). Meridional patterns in the deep scattering layers and top predator distribution in the central equatorial Pacific. *Fish. Oceanogr.* 19, 427-433.
34. Kelly, L.W., Williams, G.J., Barott, K.L., Carlson, C.A., Dinsdale, E.A., Edwards, R.A., Haas, A.F., Haynes, M., Lim, Y.W., McDole, T., et al. (2014). Local genomic adaptation of coral reef-associated microbiomes to gradients of natural variability and anthropogenic stressors. *Proceedings of the National Academy of Sciences of the United States of America* 111, 10227-10232.
35. Altabet, M.A. (2001). Nitrogen isotopic evidence for micronutrient control of fractional NO_3^- utilization in the equatorial Pacific. *Limnol. Oceanogr.* 46, 368-380.
36. Leichter, J.J., and Genovese, S.J. (2006). Intermittent upwelling and subsidized growth of the scleractinian coral *Madracis mirabilis* on the deep fore-reef slope of Discovery Bay, Jamaica. *Mar. Ecol. Prog. Ser.* 316, 95-103.
37. Palardy, J.E., Grottoli, A.G., and Matthews, K.A. (2005). Effects of upwelling, depth, morphology and polyp size on feeding in three species of Panamanian corals. *Mar. Ecol. Prog. Ser.* 300, 79-89.
38. Graham, N.A.J., Wilson, S.K., Carr, P., Hoey, A.S., Jennings, S., and MacNeil, M.A. (2018). Seabirds enhance coral reef productivity and functioning in the absence of invasive rats. *Nature* 559, 250.
39. Lewis, J.B., and Price, W.S. (1975). Feeding mechanisms and feeding strategies of Atlantic reef corals. *J. Zool.* 176, 527-544.
40. Maier, C., Weinbauer, M.G., and Pätzold, J. (2010). Stable isotopes reveal limitations in C and N assimilation in the Caribbean reef corals *Madracis auretenra*, *M. carmabi* and *M. formosa*. *Mar. Ecol. Prog. Ser.* 412, 103-112.
41. Swart, P.K., Saied, A., and Lamb, K. (2005). Temporal and spatial variation in the $\delta^{15}\text{N}$ and $\delta^{13}\text{C}$ of coral tissue and zooxanthellae in *Montastraea faveolata* collected from the Florida reef tract. *Limnol. Oceanogr.* 50, 1049-1058.
42. Porter, J.W. (1976). Autotrophy, heterotrophy, and resource partitioning in Caribbean reef-building corals. *Am. Nat.* 110, 731-742.
43. Grottoli, A.G., Warner, M.E., Levas, S.J., Aschaffenburg, M.D., Schoepf, V., McGinley, M., Baumann, J., and Matsui, Y. (2014). The cumulative impact of annual coral bleaching can turn some coral species winners into losers. *Global Change Biol.* 20, 3823-3833.
44. Leichter, J.J., Wing, S.R., Miller, S.L., and Denny, M.W. (1996). Pulsed delivery of subthermocline water to Conch Reef (Florida Keys) by internal tidal bores. *Limnol. Oceanogr.* 41, 1490-1501.
45. Leichter, J.J., Stokes, M.D., Hench, J.L., Witting, J., and Washburn, L. (2012). The island - scale internal wave climate of Moorea, French Polynesia. *J. Geophys. Res. Oceans* 117.
46. Sevadjan, J.C., McManus, M.A., Benoit-Bird, K.J., and Selph, K.E. (2012). Shoreward advection of phytoplankton and vertical re-distribution of zooplankton by episodic near-bottom water pulses on an insular shelf: Oahu, Hawaii. *Cont. Shelf. Res.* 50, 1-15.
47. Baumann, J., Grottoli, A.G., Hughes, A.D., and Matsui, Y. (2014). Photoautotrophic and heterotrophic carbon in bleached and non-bleached coral lipid acquisition and storage. *J. Exp. Mar. Biol. Ecol.* 461, 469-478.

48. Houlbrèque, F., and Ferrier-Pagès, C. (2009). Heterotrophy in tropical scleractinian corals. *Biol Rev Camb Philos Soc* 84, 1-17.
49. Levas, S.J., Grottoli, A.G., Hughes, A., Osburn, C.L., and Matsui, Y. (2013). Physiological and biogeochemical traits of bleaching and recovery in the mounding species of coral *Porites lobata*: implications for resilience in mounding corals. *PloS one* 8, e63267.
50. Anthony, K.R.N., Hoogenboom, M.O., Maynard, J.A., Grottoli, A.G., and Middlebrook, R. (2009). Energetics approach to predicting mortality risk from environmental stress: a case study of coral bleaching. *Funct. Ecol.* 23, 539-550.
51. Wooldridge, S.A. (2009). Water quality and coral bleaching thresholds: Formalising the linkage for the inshore reefs of the Great Barrier Reef, Australia. *Mar. Pollut. Bull.* 58, 745-751.
52. Wiedenmann, J., D'Angelo, C., Smith, E.G., Hunt, A.N., Legiret, F.-E., Postle, A.D., and Achterberg, E.P. (2012). Nutrient enrichment can increase the susceptibility of reef corals to bleaching. *Nat. Clim. Chang.* 3, 160-164.
53. Wooldridge, S.A. (2016). Excess seawater nutrients, enlarged algal symbiont densities and bleaching sensitive reef locations: 1. Identifying thresholds of concern for the Great Barrier Reef, Australia. *Mar. Pollut. Bull.*
54. Duprey, N.N., Yasuhara, M., and Baker, D.M. (2016). Reefs of tomorrow: Eutrophication reduces coral biodiversity in an urbanized seascape. *Global Change Biol.* 22, 3550-3565.
55. Williams, G.J., Gove, J.M., Eynaud, Y., Zgliczynski, B.J., and Sandin, S.A. (2015). Local human impacts decouple natural biophysical relationships on Pacific coral reefs. *Ecography* 38, 751-761.
56. Karnauskas, K.B., and Cohen, A.L. (2012). Equatorial refuge amid tropical warming. *Nat. Clim. Chang.* 2, 530-534.
57. Karnauskas, K.B., Cohen, A.L., and Gove, J.M. (2016). Mitigation of Coral Reef warming across the Central Pacific by the equatorial undercurrent: a past and future divide. *Sci. Rep.* 6.
58. Riegl, B., Glynn, P.W., Wieters, E., Purkis, S., d'Angelo, C., and Wiedenmann, J. (2015). Water column productivity and temperature predict coral reef regeneration across the Indo-Pacific. *Sci Rep* 5, 8273.
59. Wall, M., Putchim, L., Schmidt, G.M., Jantzen, C., Khokiattiwong, S., and Richter, C. (2015). Large-amplitude internal waves benefit corals during thermal stress. *Proc. R. Soc. B.* 282, 20140650.
60. Smith, J.E., Brainard, R., Carter, A., Grillo, S., Edwards, C., Harris, J., Lewis, L., Obura, D., Rohwer, F., and Sala, E. (2016). Re-evaluating the health of coral reef communities: baselines and evidence for human impacts across the central Pacific. *Proc. R. Soc. B* 283, 20151985.
61. Johnston, E.C., Forsman, Z.H., Flot, J.-F., Schmidt-Roach, S., Pinzón, J.H., Knapp, I.S.S., and Toonen, R.J. (2017). A genomic glance through the fog of plasticity and diversification in *Pocillopora*. *Sci. Rep.* 7, 5991.
62. Williams, G.J., Knapp, I.S., Maragos, J.E., and Davy, S.K. (2010). Modeling patterns of coral bleaching at a remote Central Pacific atoll. *Mar. Pollut. Bull.* 60, 1467-1476.
63. Williams, G.J., Smith, J.E., Conklin, E.J., Gove, J.M., Sala, E., and Sandin, S.A. (2013). Benthic communities at two remote Pacific coral reefs: effects of reef habitat, depth, and wave energy gradients on spatial patterns. *PeerJ* 1, e81.

64. Williams, I.D., Baum, J.K., Heenan, A., Hanson, K.M., Nadon, M.O., and Brainard, R.E. (2015). Human, Oceanographic and Habitat Drivers of Central and Western Pacific Coral Reef Fish Assemblages. PLoS ONE 10, e0120516.
65. Hughes, A.D., Grottoli, A.G., Pease, T.K., and Matsui, Y. (2010). Acquisition and assimilation of carbon in non-bleached and bleached corals. Mar. Ecol. Prog. Ser. 420, 91-101.
66. Nahon, S., Richoux, N.B., Kolasinski, J., Desmalades, M., Pages, C.F., Lecellier, G., Planes, S., and Lecellier, V.B. (2013). Spatial and temporal variations in stable carbon ($\delta^{13}\text{C}$) and nitrogen ($\delta^{15}\text{N}$) isotopic composition of symbiotic scleractinian corals. PloS One 8, e81247.
67. Grottoli, A.G., and Wellington, G.M. (1999). Effect of light and zooplankton on skeletal $\delta^{13}\text{C}$ values in the eastern tropical Pacific corals *Pavona clavus* and *Pavona gigantea*. Coral Reefs 18, 29-41.
68. Moran, R., and Porath, D. (1980). Chlorophyll determination in intact tissues using N,N-Dimethylformamide. Plant Physiol. 65, 478-479.
69. Wellburn, A.R. (1994). The spectral determination of chlorophylls a and b, as well as total carotenoids, using various solvents with spectrophotometers of different resolution. J. Plant Physiol. 144, 307-313.
70. Stimson, J., and Kinzie, R.A. (1991). The temporal pattern and rate of release of zooxanthellae from the reef coral *Pocillopora damicornis* (Linnaeus) under nitrogen-enrichment and control conditions J. Exp. Mar. Biol. Ecol. 153, 63-74.
71. Zar, J.H. (2007). Biostatistical Analysis, Fifth Edition, (New Jersey: Prentice-Hall, Inc.).
72. Bates, D., Mächler, M., Bolker, B.M., and Walker, S. (2015). Fitting linear mixed-effects models using lme4. J. Stat. Software 67, 1-48.
73. Barton, K. (2015). MuLIn: Multi-Model Inference. R Package version 1.13.4.
74. Hurvich, C.M., and Tsai, C. (1989). Regression and time series model selection in small samples. Biometrika 76, 297-307.
75. Rebert, J.P., Donguy, J.R., Eldin, G., and Wyrski, K. (1985). Relations between sea level, thermocline depth, heat content, and dynamic height in the tropical Pacific Ocean. J. Geophys. Res. Oceans 90, 11719-11725.
76. Lindell, D., and Post, A.F. (1995). Ultraphytoplankton succession is triggered by deep winter mixing in the Gulf of Aqaba (Eilat), Red Sea. Limnol. Oceanogr. 40, 1130-1141.

Figure Legends

Figure 1. Oceanographic climate of the Southern Line Islands.

A Satellite-derived climatological means of surface chlorophyll-*a* in the Southern Line Islands from 2004-2015. **B** Boxplot of annual mean chl-*a* concentrations calculated for each of the most proximate pixels to an island. The box represents lower and upper quartiles with the median value shown as a black line. Whiskers represent the minimum and maximum values that are not greater than 1.5 times the difference between the upper and lower quartiles. All data beyond this limit are displayed as points. **C** Mean inorganic nutrient concentrations across all depths (5, 10, 15, 25, 30 m; *n*=3 per depth). Error bars are \pm 1SE. For dissolved inorganic nitrogen (DIN), letters denote significant differences at the $p < 0.05$ level and for soluble reactive phosphorus (SRP) differences are denoted with i or ii. **D** Mean differences between coral host and zooplankton $\delta^{13}\text{C}$ ($\Delta^{13}\text{C}_{\text{coral-zooplankton}}$) across the SLI as a function of mean surface chl-*a*. All data are from corals at 10 m (*n*=5) and the zooplankton values were calculated as the mean of duplicate samples from three different sites on the leeward coast (*n*=3) of each island. The line represents best-fit linear regression ($p < 0.01$, $r^2 = 0.94$) and the shaded region represents \pm 1SE of the linear fit. See also Figure S1.

Figure 2. *Pocillopora meandrina* host and endosymbiont $\delta^{13}\text{C}$ and $\Delta^{13}\text{C}$ across depth in the SLI.

Islands are ordered top to bottom from north to south, in order of decreasing surface chl-*a*. Data are presented for depths 5-30 m in 5 m intervals (*n*=6 per island) In plots **A-E**, the lines are provided to help visualize the relationship between tissue $\delta^{13}\text{C}$ and depth in the coral host (solid) and endosymbiont (dashed) fractions. In plots **F-J** the dashed line represents $\Delta^{13}\text{C}$ ($\delta^{13}\text{C}_{\text{host}} - \delta^{13}\text{C}_{\text{endosymbiont}}$) = 0, or no difference in $\delta^{13}\text{C}$ between coral host and endosymbiont tissues. All data points and error bars represent mean values \pm 1SE (*n* = 5) except for Flint 30 m (*n* = 3). Lines of best fit are displayed for significant linear regressions of $\Delta^{13}\text{C}$ as a function of depth at each island. Shaded areas represent \pm 1SE of the linear fit and error bars represent \pm 1SE of the mean. See also Figure S1 and Table S1-2.

Figure 3. Global patterns of coral and endosymbiont $\delta^{13}\text{C}$ and $\Delta^{13}\text{C}$ as a function of surface chl-*a*.

A Locations from the global data set are depicted in the maps with the first three to four letters of each location corresponding to the island name in the magnified regions for the (a) Maldives, (b) central Pacific, and (c) Caribbean basin. The Gulf of Eilat is shown only in the global map. Regions of lower surface chl-*a* are shown in blue and areas of higher surface chl-*a* in red. **B** Boxplot of annual mean surface chl-*a* data from 2004-2015 for all islands. Shaded boxes indicate the five SLI. **C** Mean coral and endosymbiont $\delta^{13}\text{C}$ as a function of surface chl-*a*. **D** Mean $\Delta^{13}\text{C}$ ($\delta^{13}\text{C}_{\text{coral}} - \delta^{13}\text{C}_{\text{endosymbiont}}$) as a function of surface chl-*a*. Mean values for Jamaica (JAM), Gulf of Eilat (EIL), and all atolls in the Maldives (except MAA) are composite means of all species sampled at that location (see Table S6 for a complete list). Chl-*a* estimates are based on data from between the 7 and 13 most proximate pixels to each sampling location and represent the climatological mean from 2004 to 2015. The line represents best-fit linear regression ($p < 0.001$, $r^2 = 0.77$) and the shaded region represents \pm 1SE of the linear fit. See also Figure S2 and Tables S3-S4.

STAR METHODS

CONTACT FOR REAGENT AND RESOURCE SHARING

Further information and requests for resources and reagents should be directed to and will be fulfilled by the Lead Contact, Michael Fox (fox@ucsd.edu).

EXPERIMENTAL MODEL AND SUBJECT DETAILS

The Southern Line Islands, of the Republic of Kiribati consist of four low-lying limestone islands (Flint, Vostok, Starbuck, and Malden) and one atoll (Millennium) (Figure 1A). These coral-dominated islands [60] represent reef ecosystems that have likely adapted to long-term differences in inorganic nutrient availability and primary production (PP) due to variation in regional oceanography in the absence of local human impacts. All research was conducted on the leeward (west) fore reef habitat of each island between October and November 2013. Sites were selected based on previously published data and were representative of island-scale averages for benthic community structure [60].

For the first part of this study, we sought to compare the trophic ecology of a common reef-building coral across a natural, long-term gradient in nearshore primary production. We chose to examine a species that is widely distributed coral throughout the Pacific and Indian oceans, *Pocillopora meandrina*. We recognize the challenges of accurately identifying *Pocillopora* species visually in the field given the high level of morphological plasticity within this genus [61]. However, the relative abundance of *P. meandrina* throughout the Line Islands [62, 63] supports our identification. We removed approximately 2-3 cm² branch tips from the top-center of five similarly sized colonies of *P. meandrina*. All sampled colonies were separated by at least 5m when abundant and collections were made strictly along the isobaths at each depth. Samples in the SLI were collected at 5, 10, 15, 20, 25, 30 m on each island and placed in individual UV protective sample bags. During transport to the research vessel, samples were stored in the dark and on ice and then frozen at -20° C until analysis.

We also examined the relationship between coral trophic ecology and nearshore primary production on a global scale using previously published coral isotope data from the literature. Coral host tissue and endosymbiont $\delta^{13}\text{C}$ and $\delta^{15}\text{N}$ values were acquired from published studies (Table S4). Only data from studies that collected corals at 10 m depth and presented independent means of host and endosymbiont fractions were included. This depth was selected because it is among the most commonly surveyed depth on fore reef habitats [60] and therefore most relevant to previous studies of coral reef benthic communities. When isotopic means were not provided in a table, values were extracted from figures using Data Thief 3.0 (www.datathief.org). If multiple coral species were sampled at the same location, their isotopic values were averaged to create a site-specific mean in order to avoid pseudoreplication among each level of chl-*a* in our statistical analyses.

METHOD DETAILS

Oceanographic context of the Southern Line Islands

To quantify differences in ambient inorganic nutrient concentrations across the SLI, triplicate water samples (50mL) were collected at 5, 10, 15, 20, and 30 m at each site, filtered (0.7 μm GF/F filters, Whatman) and frozen at -20°C until analysis. Samples were analyzed for dissolved inorganic nitrogen ($\text{DIN} = \text{NO}_3^- + \text{NO}_2^- + \text{NH}_4^+$) and soluble reactive phosphorus (SRP) at the University of Hawaii Hilo EPSCoR analytical laboratory. Inter-island variation in nutrient concentrations were compared using a two-way fixed factor analysis of variance (ANOVA) to examine the effects of island and depth and their possible interaction. Assumptions of normality and homoscedasticity were verified by using the Anderson-Darling test and Levene's test, respectively. There was significant interaction between island and depth for DIN

($F_{16,40} = 5.083$, $p < 0.001$, Figure 1C). This interaction, however, was driven by differences in nutrient concentrations at the same depths across islands. The only intra-island differences across depth occurred on Malden (Tukey HSD: 5 m < 15, 25, 30 m) and the difference was $< 0.5 \mu\text{mol}$. Phosphate concentrations did not vary with depth but differed among islands ($F_{4,40} = 70.66$, $p < 0.001$). As such, we considered inorganic nutrient concentrations to be homogenous throughout the upper 30 m and pooled the data to present an integrated mean for the water column. *In situ* photosynthetically active radiation (PAR) was recorded with a LI-COR 4π quantum sensor (LI-1400, LICOR USA) that was deployed at 10 m depth for 2-4 diel cycles at each island. The relative light environment at each island over longer time scales was assessed by determining the depth of light penetration at 490 nm (K490) from the MODIS data package, *sensu* [26].

To quantify patterns of island-scale PP we used the eight-day 0.0417° ($\sim 4\text{-km}$) spatial resolution product of chl-*a* (mg m^{-3}) derived from the Moderate Resolution Imaging Spectroradiometer (MODIS; <https://modis.gsfc.nasa.gov/>). Data were obtained for 2004-2015 (12 years) to provide climatological means of surface chl-*a* concentrations across the SLI, *sensu* [6]. Briefly, pixels that fell within 3.27 km of the 30 m isobath of each island were excluded to avoid data confounded by optically shallow water. Next, a full pixel width (4.4 km) buffer region was extended beyond the 3.27 km exclusion zone and used to select a single band of pixels around each island. These pixels were averaged to create island-scale climatological estimates of chl-*a* concentrations as a proxy for nearshore PP and heterotrophic resource availability.

The mean number of pixels used around the smallest oceanic islands in this study (Palmyra Atoll and all islands in the SLI) was 13. Therefore, climatological chl-*a* estimates were derived for other locations using the mean of the 13 most proximate pixels along shore of the collection site. This standardized the spatial areas considered for the PP climatologies at each

location and allowed for more ecologically relevant estimates along continental coastlines such as in the Red Sea or from large islands, such as Jamaica.

By using chl-*a* data from optically clear waters we avoid confounding data from nearshore waters that may be influenced by terrestrial runoff or other anthropogenic impacts [31]. Consequently, our chl-*a* estimates are not made on the reef and may therefore underestimate the overall chl-*a* concentration and plankton abundance. However, this proxy to nearshore primary production is a powerful predictor of the biological responses of coral reef communities, most notably corals and planktivorous fish [55, 64]. Satellite-derived chl-*a* estimates from 29 Pacific islands also accurately reflect phytoplankton biomass throughout the euphotic zone [26]. The mean chl-*a* concentration at each island during our cruise in October-November 2013 mirrored the long-term climatologies for the region and was strongly correlated with *in situ* DIN concentrations ($r = 0.97$). Thus, we believe that remotely sensed chl-*a* accurately reflect surface chl-*a* conditions near coral reef environments over longer time scales and that this metric provides a relevant estimate of food abundance for coastal mixotrophs in the tropics.

Stable isotope analysis of Pocillopora across islands and depths in the SLI

Coral host and endosymbiont fractions were isolated following established methods [18, 23, 24, 65]. An airbrush was used to remove tissue from the skeleton using 10 mL of 0.07 μ m filtered seawater (FSW). The resulting blastate was homogenized with an electric tissue homogenizer. The animal fraction was isolated through centrifugation at 2,000g for 5 min to pellet most of the endosymbionts. The supernatant (animal fraction) was decanted and the symbionts fraction was suspended in 2 mL of FSW, centrifuged again. The supernatant from this

was added to the animal fraction, which was centrifuged a final time to pellet any residual endosymbionts and 2 mL were loaded onto a pre-combusted GF/F filter (Whatman). To minimize the contamination of the endosymbiont fraction by coral host tissue (and therefore optimize our ability to detect true heterotrophic signals), the endosymbiont fraction was then resuspended in 5 mL FSW, pressure filtered through 83 and 20 μm nitex mesh and pelleted at 2,000 g. This filtration was repeated once more before 1 mL of the endosymbiont fraction was loaded onto a pre-combusted GF/F. Each sample was briefly rinsed with 1mL 1N HCl to remove calcium carbonate from the coral sample and rinsed with 1 mL of DI water [66]. Acidified and non-acidified samples were tested against each other to ensure that rinsing with a weak acid did not affect nitrogen isotope values. We examined acidification effects on both tissue fractions (n=5) using paired t-tests and found no effect of this light acidification on $\delta^{15}\text{N}$ of either tissue type ($t_{\text{host}}=1.50$, $p=0.21$; $t_{\text{symbiont}}=-0.08$, $p=0.94$). No differences were observed for $\delta^{13}\text{C}$ either; suggesting CaCO_3 contamination is minimal following this protocol with *P. meandrina* ($t_{\text{host}}=-1.69$, $p=0.17$; $t_{\text{symbiont}}=-0.42$, $p=0.69$). The mean offset between acidified and non-acidified samples were: $\delta^{13}\text{C}_{\text{host}}=-0.02 \pm 0.02 \text{ ‰}$, $\delta^{15}\text{N}_{\text{host}}=-0.01 \pm 0.02 \text{ ‰}$, $\delta^{13}\text{C}_{\text{symbiont}}=-0.03 \pm 0.15 \text{ ‰}$, $\delta^{15}\text{N}_{\text{symbiont}}=-0.03 \pm 0.02 \text{ ‰}$. As such, we elected to briefly acidify each sample to minimize the risk of CaCO_3 contamination and $\delta^{13}\text{C}$ and $\delta^{15}\text{N}$ were determined from the same sample.

The isolated fractions were analyzed for $\delta^{13}\text{C}$, $\delta^{15}\text{N}$ and $\mu\text{g C:N}$ with a Costech 4010 Elemental Combustion Analyzer interfaced with a Thermo Finnigan Delta Plus XP stable isotope mass spectrometer (San Jose, CA) at Scripps Institution of Oceanography. Isotopic values are expressed as $\delta^{13}\text{C}/^{15}\text{N}$, where $\delta = 1000 \times [(R_{\text{sample}} / R_{\text{standard}}) - 1]$ and R_{sample} or R_{standard} are the ratio of the heavy to light isotope in parts per thousand, or per mil (‰). The $\text{C}^{13}/\text{C}^{12}$ and $\text{N}^{15}/\text{N}^{14}$ ratios are expressed relative to the levels of ^{13}C in Vienna-Pee Dee Belemnite (V-PDB) and ^{15}N in

atmospheric N₂. Repeated measurements (n=60) of internal working standards exhibited a precision of 0.01‰ for $\delta^{13}\text{C}$ and 0.2‰ for $\delta^{15}\text{N}$. The internal standards of calcium carbonate and ammonium sulfate were calibrated against NBS 18 and IAEA-1, respectively. Ten percent of all samples (n=18) were run in duplicate with a measurement error $\pm 0.12\text{‰}$ for $\delta^{13}\text{C}$ and $\pm 0.31\text{‰}$ for $\delta^{15}\text{N}$.

The amount of heterotrophic carbon incorporated by *Pocillopora* was inferred by calculating the difference between the $\delta^{13}\text{C}$ values of the coral host and endosymbiont fractions ($\Delta^{13}\text{C} = \delta^{13}\text{C}_{\text{host}} - \delta^{13}\text{C}_{\text{endosymbiont}}$) [23]. This metric has been shown to accurately track intra-island variations in resource availability across sites and depth in this coral species within the Line Islands [24]. To verify that the dominant coral food sources (e.g. zooplankton and particulate organic matter (POM)) had more negative $\delta^{13}\text{C}$ values than the coral host and endosymbiont tissue [23, 67] (to ensure accurate interpretation of the $\Delta^{13}\text{C}$ metric), we collected reef-associated POM (2 L seawater filtered onto 25 mm GF/F) and zooplankton (>133 μm , collected across full diel cycles using an autonomous plankton sampler, *sensu* [24]) from 10 m depth at 3 leeward sites per island. Both sample types were concentrated on pre-combusted GF/F filters and briefly acidified as above. For each zooplankton filter (n=3 per island), duplicate subsamples were averaged together to account for the heterogeneous distribution of plankton across the filter.

To extract chlorophyll-*a*, endosymbionts were pelleted from 2 mL of coral blastate from each coral at 10, 20, and 30 m. The animal fraction was decanted and the algal pellet was homogenized in 1 mL in *N,N*-dimethylformamide (DMF) and the pigments were extracted for 24 hrs at 4 °C following [68]. The sample was then centrifuged for 5 min at 7,000 x g to remove all particulate debris and the supernatant was analyzed with a diode array spectrophotometer

(Agilent, UV-vis 8453) following the equations of [69] for a spectrophotometer with 1 nm resolution. Pigment concentrations were normalized to surface area of each coral fragment determined by wax dipping [70], initial blastate volume, and solvent volume. Endosymbiont density was quantified by 6 replicate counts on a Hausser hemocytometer and normalized to initial blastate volume and coral surface area.

QUANTIFICATION AND STATISTICAL ANALYSIS

To determine if coral host tissue was more similar to its dominant prey source (zooplankton) on more productive islands, we examined the difference between the coral host tissue with zooplankton $\delta^{13}\text{C}$ and $\delta^{15}\text{N}$ values at each island using only corals from 10 m (to be consistent with the depth of zooplankton collections). We used a one-way ANOVA to test for differences in zooplankton $\delta^{13}\text{C}$ among islands. Assumptions of normality and homoscedasticity were verified by using the Anderson-Darling test and Levene's test, respectively. Zooplankton $\delta^{13}\text{C}$ did not vary among islands ($F_{(4,10)} = 1.59$, $p = 0.5$) so we used island-specific zooplankton $\delta^{13}\text{C}$ values to examine the relationship between coral host and zooplankton $\delta^{13}\text{C}$ ($\Delta^{13}\text{C}_{\text{host-zooplankton}}$). We used a standard linear model to assess the relationship between $\Delta^{13}\text{C}_{\text{host-zooplankton}}$ and $\Delta^{15}\text{N}_{\text{host-zooplankton}}$ as a function of surface chl-*a* at each island.

Spatial variability in $\delta^{13}\text{C}$, $\delta^{15}\text{N}$, and C:N and their relative differences between tissue fractions (Δ) across depths and islands was examined using an analysis of covariance (ANCOVA) on mean values ($n=5$ per depth except Flint 30 m, $n=3$) to account for non-independence among replicate samples within each level of depth. Assumptions of normality and homoscedasticity were verified by using the Anderson-Darling test and Levene's test, respectively. We included depth as a covariate to test for differences in the slope of the relationship between tissue chemistry and depth across the SLI (significant interaction term) and

for differences in the magnitude of the heterotrophic signal (significant effect of island). Significant differences in the slopes of island-specific regressions of mean values vs. depth were determined individually in pairwise contrasts [71].

Coral pigment content was log transformed to satisfy the assumptions of normality and homoscedasticity and compared across islands and depth with a two-way fixed factor ANOVA. The relationship between coral pigment content and endosymbiont density and their respective influence on coral $\Delta^{13}\text{C}$ was examined using Pearson's correlations for all coral samples from 10 m pooled across the SLI (n=25).

Global relationships between coral isotopic ratios and nearshore primary production

The physiology and trophic strategies of scleractinian corals vary considerably across taxa [29]. We acknowledge that averaging the $\Delta^{13}\text{C}$ estimates of multiple species reduces our ability to examine species-specific patterns and intra-site variability, but this allowed us to test our observed relationship in the most statistically rigorous fashion. To account for the influence of coral taxonomy on our observed relationship between $\Delta^{13}\text{C}$ and surface chl-*a*, we refined the global dataset to only include data from coral families that were replicated in at least two separate locations (intra-archipelago replication excluded). The resulting dataset thus excluded samples from the Acroporidae and Meandrinidae (Jamaica) and Oculinidae (Maldives) families from the mean $\Delta^{13}\text{C}$ estimates at those locations. The resulting family-level dataset contained $\Delta^{13}\text{C}$ estimates from all 16 locations but only for corals from four families (Agariciidae, Astrocoeniidae, Faviidae, Pocilloporidae). Using this refined dataset, we tested the consistency of our observed linear relationship between $\Delta^{13}\text{C}$ and chl-*a* at both island and regional scales.

To examine the influence of spatial autocorrelation on heterotrophy estimates from geographically clustered islands, we fitted a linear mixed effects model (lme4 package for R [72]) with region included as a random effect (model 1) on the intercept as: $\text{mean } \Delta^{13}\text{C} \sim \text{mean chl-}a + (1|\text{Region})$. Region explained zero percent of the model variance while surface chl-*a* was a significant predictor variable ($p < 0.01$, $r^2 = 0.78$). To further address this concern, we compared the performance of this model with a standard general linear model (model 2) (residuals of our data were normally distributed, were not auto-correlated, and showed no sign of heteroscedasticity) using Akaike Information Criterion (MuMIn package [73]) corrected for small sample size AICc [74]. Both models confirmed that chl-*a* was a significant predictor variable and indicated that the effect of surface chl-*a* concentration on coral $\Delta^{13}\text{C}$ was consistent within and across regions, regardless of ocean basin ($p < 0.01$). The slope and y-intercept of both models were identical; therefore we selected the more parsimonious general linear model of island means as the model of best fit ($\Delta\text{AICc} = -5.19$ relative to model 1).

To test for a spatial bias driven by uneven sampling within individual regions (1-6 islands per archipelago), we collapsed the island-mean estimates of heterotrophy into regional means (i.e. data from each island of an archipelago were averaged, thereby reducing the influence of spatial autocorrelation within archipelagos). Our expectation was that significant regional bias would reduce performance of the regional general linear model (model 3). Notably, this approach had no significant effect on model performance (model 2: $F_{1,14} = 44.44$, $r^2 = 0.77$, $p < 0.001$; model 3: $F_{1,5} = 18.35$, $r^2 = 0.79$, $p = 0.01$). Therefore, we used the standard general linear model of island-specific $\Delta^{13}\text{C}$ estimates to most accurately capture the variation across all 16 locations.

To further assess the performance of our selected linear model we performed a sensitivity analysis to assess the influence of taxonomy and geography on model performance by reducing the model in a step-wise fashion (Table S3). First, we tested for a significant relationship between surface chl-*a* and all coral $\delta^{13}\text{C}$ and $\Delta^{13}\text{C}$ data for 15 species. Next, we removed islands whose mean $\Delta^{13}\text{C}$ value was created from multiple species (i.e., Jamaica, Eilat) and for a species with uniquely deplete $\delta^{13}\text{C}$, *Madracis spp.* [23]. Then, we further reduced the model to include only data from a single species at all locations (excluding Jamaica and using *Stylophora pistillata* from the Gulf Eilat due to its genetic relatedness to *Pocillopora*). Finally, we examined the most simplistic model, only $\delta^{13}\text{C}$ and $\Delta^{13}\text{C}$ data for *Pocillopora* from the Line Islands and the Maldives. We calculated coefficients of variation for the slope and y-intercept terms across all models (excluding model with raw data) to assess overall variation. See Table S3 for statistical summaries of each model, respectively.

Finally, to disentangle the influence of geography vs. oceanographic processes related to resource availability (i.e., PP and upwelling) on coral and endosymbiont $\delta^{13}\text{C}$ and $\delta^{15}\text{N}$ values we examined linear relationships between absolute latitude (as a proxy for light and temperature) and estimated thermocline depth (as a proxy for resource delivery potential, as internal wave delivery of subthermocline resources are more probable in regions with shallower thermoclines [75]). Thermocline depth was estimated as the depth of the 22° isotherm computed using objectively analyzed mean SST averaged across all available decades from the World Ocean Atlas (<https://www.nodc.noaa.gov/OC5/woa13/>). Thermocline depth in the tropical Pacific is well estimated by the depth of the 20° isotherm [75], however, we used the 22° isotherm in order to include the Gulf of Eilat in our analysis, which can be mixed to depths in excess of 600 m [76] and did not go below 22° in the world ocean atlas database. Mean temperatures from the surface

to 1000m were determined for each island in the global dataset using a horizontal average of a 1° x 1° box centered on each island [24]. Depth of the 22° isotherm was estimated from linear fits of temperature vs. depth for a temperature of $14-28^\circ$ ($r^2 > 0.95$ for all models), which provided independent estimates of thermocline depth for each location. To account for the geographic proximity of several atolls in the Maldives, the atolls from this region were consolidated into north, central, and south groups (isotope data averaged across two atolls per region). Thus, the degrees of freedom in this analysis differed slightly from the global model presented above (df = 11 vs. 13). We compared linear models (Table S4) based on mean isotope values as described above. We also examined coral and endosymbiont $\delta^{15}\text{N}$ and $\Delta^{15}\text{N}$ across the Pacific and Indian oceans and for only *Pocillopora* from the Line Islands and the Maldives to control for regional oceanographic differences and elucidate how oceanic ^{15}N baselines influence coral $\delta^{15}\text{N}$. All statistical analyses were completed using R (R Core Team 2013 and related packages).

DATA AND SOFTWARE AVAILABILITY

The datasets generated during and/or analyzed during this study have been deposited in the Mendeley Data repository at: <http://doi:10.17632/dhvyrxcxhw.1> The data sets we have deposited include: Annual surface chl-*a* concentrations determined for each location in the global analysis, *Pocillopora* host and endosymbiont $\delta^{13}\text{C}$, $\delta^{15}\text{N}$, C:N data from the Southern Line Islands, Inorganic nutrient concentrations from the Southern Line Islands, and Sea Surface Temperature data for upper 1000 m from the World Ocean's Atlas

Figure 1

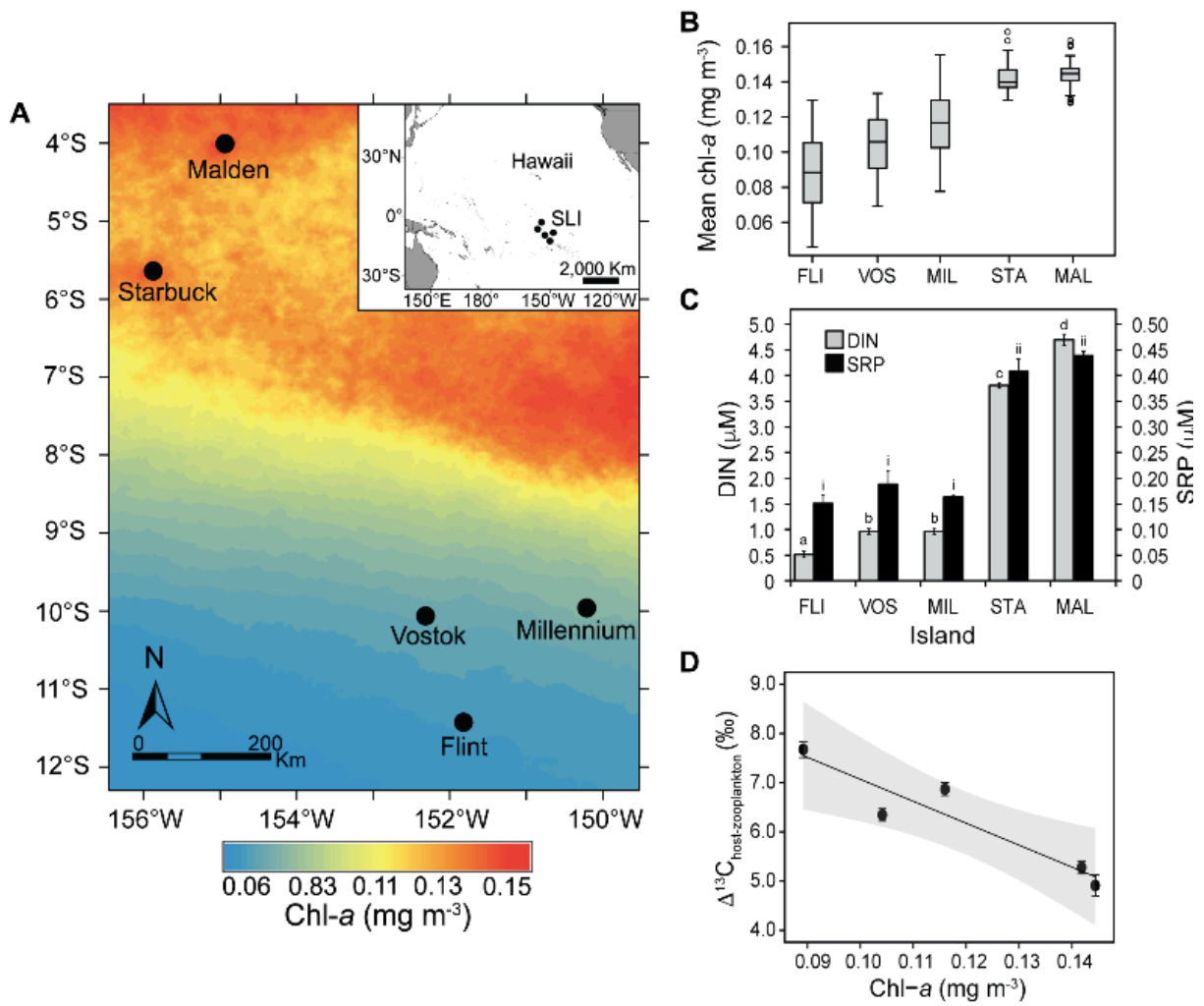
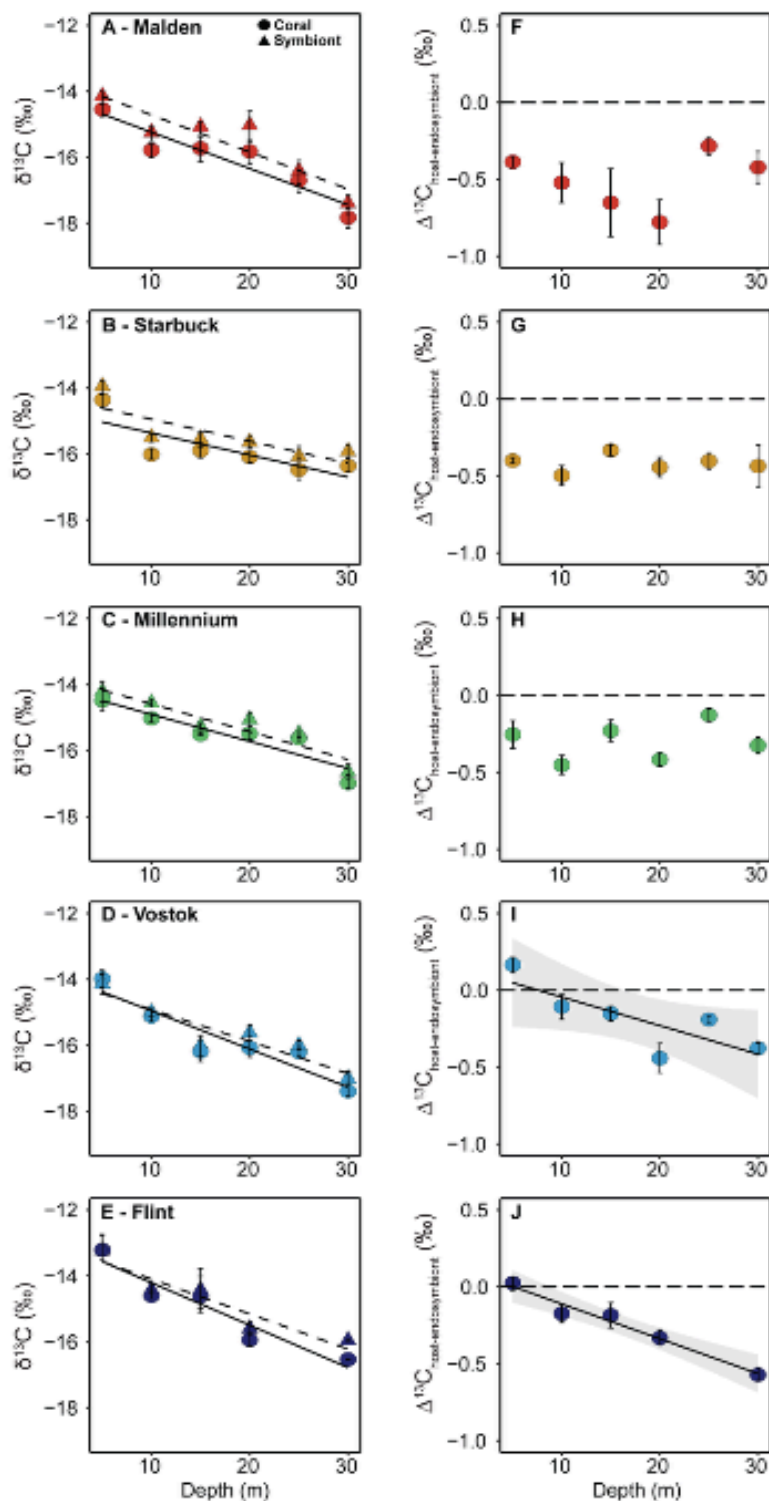
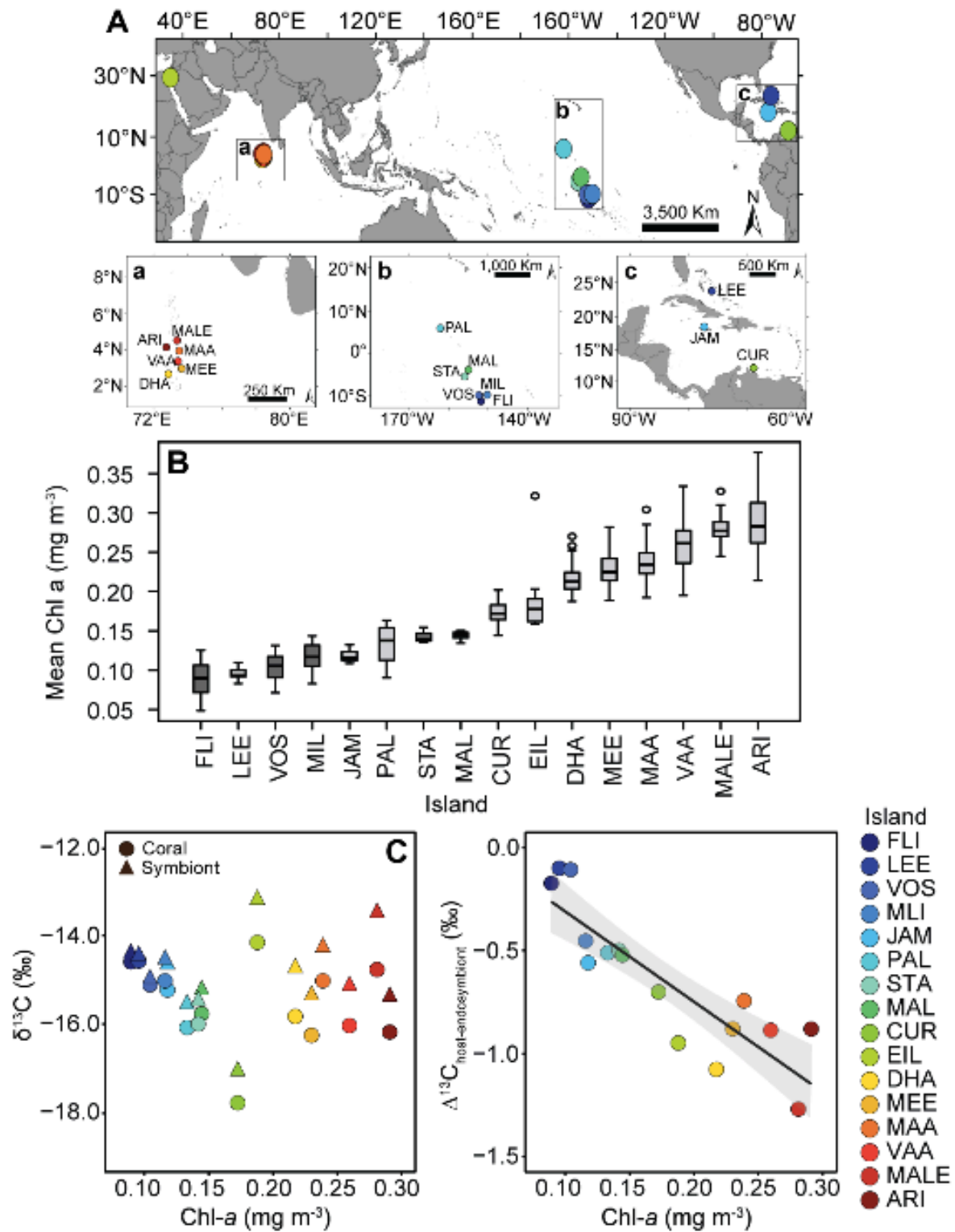


Figure 2



935 Figure 3
936



937